Table 1. Variation of $|E_+'/A_1|$ with ω_1/ω_2 and λ_w

ω_1/ω_2	λ_w (cm)	$\lvert E_+'/A_1\rvert$
1.5	1.47	0.12
2	1.07	0.17
2.5	0.89	0.23
3	0.76	0.29

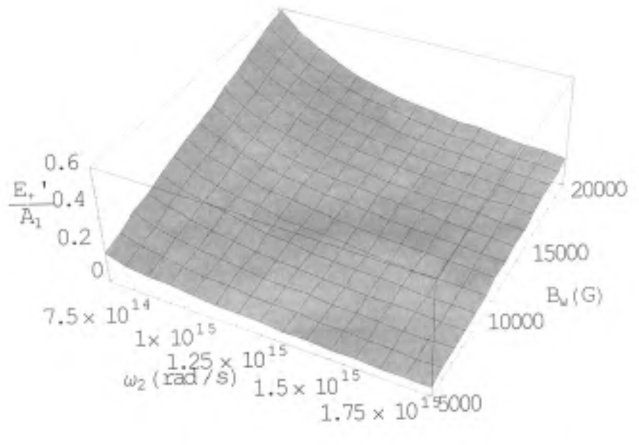

Figure 3. Variation of $|E_+'/A_1|$ with the frequency of the second laser ω_2 and wiggler field strength B_w.

For a typical case of *n*-type germanium with electron density 10^{17} cm^{-3}, $\varepsilon_L = 14$, $\nu = 2\times10^{11}$ s^{-1}, $m = 0.3\ m_0$, $m_0 = 9.1\times10^{-28}$ g, second laser with power 2×10^6 W/cm^2, $\omega_1 = 1.8\times10^{15}$ rad/s (Nd : YAG laser), $B_w = 10$ kG, the variation of $|E_+'/A_1|$ with ω_2 and λ_w (wiggler period) is shown in the Table 1. The variation $|E_+'/A_1|$ with ω_2 and B_w is shown in Figure 3. The required wiggler wavenumber falls with plasma density and sum frequency. At higher values of plasma density the required wiggler period attains impractically smaller values. The scheme is useful in low-density plasmas and semiconductors where the amplitude of the density oscillations is not large. Employing a stronger wiggler magnetic field as well as a guide magnetic field can increase the efficiency. The estimated efficiency of the process is only an upper bound as laser propagation through plasmas and semiconductors is affected by a variety of processes, viz. insertion losses, parametric instabilities, diffraction, divergence and other nonlinear effects. In the present analysis the effect of wiggler imperfections has not been considered, which can play an important role in the generation of harmonics[14].

1. Ulmer, T. G., Hanna, M., Washburn, B. R., Ralph, S. E. and Spring Thorpe, A. J., Microactivity enhanced surface emitted second harmonic generation for ultrafast all optical signal processing. *IEEE J. Quantum Electron.*, 2002, **38**, 19–30.
2. Shen, H. M., Plasma waveguide: A concept to transfer electromagnetic energy in space. *J. Appl. Phys.*, 1991, **69**, 6827–6835.
3. Lindl, J. D., Development to the indirect drive approach to inertial confinement fusion and the target physics basis for ignition and gain. *Phys. Plasmas*, 1995, **2**, 3933–4024.
4. Van Driel, H. M., Sipe, J. E. and Young, J. F., Laser induced periodic surface structures on solids: A universal phenomenon. *Phys. Rev. Lett.*, 1982, **49**, 1955–1958.
5. Bloembergen, N., *Nonlinear Optics*, Benjamin, New York, 1965.
6. Kruer, W. L., Interaction of plasmas with intense lasers. *Phys. Plasmas*, 2000, **7**, 2270–2278.
7. Federici, J. F., Review of four wave mixing and phase conjugation in plasmas. *IEEE Trans. Plasma Sci.*, 1991, **19**, 549–564.
8. Liu, C. S. and Tripathi, V. K., Fast and slow plasma waves excitation by counter propagating lasers in a hot plasma. *Phys. Plasmas*, 2002, **9**, 3995–3998.
9. Parashar, J., Tunnel ionization due to the plasma wave produced by beating two lasers in a plasma embedded by high Z impurities. *Phys. Lett. A*, 2002, **297**, 423–426.
10. D'Ottavi, A. *et al.*, Four wave mixing in semiconductor optical amplifiers: A practical tool for wavelength conversion. *IEEE J. Sel. Top. Quantum Electron.*, 1997, **3**, 522–528.
11. Moore, G. T., Resonant sum frequency generation. *IEEE J. Quantum Electron.*, 2002, **38**, 12–18.
12. Marshall, T. C., *Free Electron Lasers*, MacMillan, New York, 1985.
13. Liu, C. S. and Tripathi, V. K., *Interaction of Electromagnetic Waves with Electron Beams and Plasmas*, World Scientific, Singapore, 1994.
14. Zhong, X. and Kong, M. C., Strong wiggler field assisted amplification in a second harmonic waveguide free electron laser. *IEEE Trans. Plasma Sci.*, 2002, **30**, 630–638.

ACKNOWLEDGEMENTS. This work was supported by AICTE, Govt. of India.

Received 15 March 2003; revised accepted 3 November 2003

On solving Schrödinger equation for the ground state of a two-electron atom using genetic algorithm

Rajendra Saha[†] and S. P. Bhattacharyya*

Department of Physical Chemistry, Indian Association for the Cultivation of Science, Jadavpur, Kolkata 700 032, India
[†]Present address: Haldia Government College, P.O. Debhog, West Bengal 721 657, India

A recipe is proposed for solving the radial Schrödinger equation (SE) for ground state of helium atom using genetic algorithm. A fitness landscape is generated and the problem of solving the radial SE is reduced to a search for the maximum on this landscape.

THE use of genetic algorithms (GAs)[1,2] for solving the Schrödinger equation (SE) numerically, is of contemporary origin[3–9]. The primary motivation has been to look

*For correspondence. (e-mail: pcspb@mahendra.iacs.res.in)

for a viable basis-set-free technique of solving the SE and generating optimal numerical wave functions. Indeed, much of quantum chemistry is dominated by the quality of basis sets, independent of whether one is using the Hartree–Fock, multiconfiguration Hartree–Fock, configuration interaction or coupled cluster methods. GA-based techniques, if proved viable, can change the scenario, for accurate numerical wave functions of atoms and few electron molecules could pave the way for designing optimal basis functions for different chemical environments. Secondly, GA is inherently parallelizable and can be therefore rather cost-effective. The basic philosophy of the method is to recast the energy eigenvalue problem in the form of a search for a global maximum on a defined fitness landscape. The targetted solution wave functions are defined as discrete functions representing the distribution of probability amplitudes in the coordinate space. A population of such wave function strings is created to start with and is made to evolve on the fitness landscape under the action of appropriately constructed genetic operators like selection, crossover, mutation, etc. In our formulation, the amplitudes are floating-point numbers and the wave functions are strings of floating-point numbers. The strings are normalized and obey appropriate boundary conditions of the problem.

The radial SE for He atom reads,

$$H\psi_n(r_1, r_2) = E_n\psi_n(r_1, r_2),$$

where

$$H = -\frac{\hbar^2}{2m_e}\sum_{i=1,2}\left(\frac{\partial^2}{\partial r_i^2}+\frac{2}{r_i}\frac{\partial}{\partial r_i}\right)-\sum_{i=1,2}\frac{ze^2}{r_i}+\frac{e^2}{r_{12}}. \quad (1)$$

From a definition of the Hamiltonian, it is evident that we are taking into account only radial correlation, leaving out the angular correlation altogether. The target is to reach the S-limit form of $\psi_0(r_1, r_2)$.

We represent ψ on a uniformly discretized two-dimensional coordinate space by n strings $(s_1, s_2, s_3, \ldots, s_k, \ldots, s_n)$, each string representing a collection of probability amplitudes $[s(i, j)]$ in a two-dimensional array of $n_1 \times n_2$ grid points. The square of $s(i, j)$ denotes the probability of finding one electron at r_1^i, while the other is at r_2^j, irrespective of spin. The permutation symmetry of the wave function ψ now needs to be considered. Since helium ground state is spin-singlet ($^1s_0$), the space part of the ground-state wave function of He $[\psi(r_1, r_2)]$ must be symmetric with respect to interchange of the coordinates of electrons 1 and 2. Therefore, the wave function strings are made to obey the following condition:

$$S_k(r_1^i, r_2^j) = S_k(r_2^i, r_1^j),\ k = 1, 2, \ldots, n. \quad (2)$$

The fitness landscape is generated by defining a fitness function (f_k) for the kth string as follows:

$$f_k = e^{-\sigma\ _k}, \quad (3)$$

where

$$_k = \left\{\frac{\langle\psi_k | H | \psi_k\rangle}{\langle\psi_k | \psi_k\rangle} - E_l\right\}^2. \quad (4)$$

σ is essentially a scaling parameter that takes care of dimensional requirements and prevents exponential overflow or underflow. E_l may be kept fixed, if a good estimate of lower bound is available or may be updated ($E_l^{i+1} = E_l^i \pm c\sqrt{\ _i}$, $c = 0.25$–0.75). For actual calculation, ψ_k in eq. (4) is replaced by the string S_k and the integrations are replaced by multidimensional quadrature. E_l is an estimated lower bound to the energy of the kth string. Fitness values for all the n strings are calculated and each string is subjected to a fitness-proportional roulette wheel selection procedure[2] that allows more copies of the better-solution string to pass into the mating pool. The average fitness of the population increases after selection – but no new information is created at this stage. For creating new information or new strings, two kinds of genetic operators are invoked, viz. crossover and mutation – the former occurring with a probability p_c and the latter with p_m. Let the strings s_k and s_l be randomly selected with probability p_c for undergoing crossover and let the ith row and the jth column of the arrays s_k, s_l be selected for crossover again with probability p_c. As a result of this operation, a pair of new strings – the children strings s_k' and s_l' are created, where

$$\left.\begin{aligned} S_k'(p,q) &= f\ S_k(p,q) + (1-f)(S_l(p,q)\\ S_l'(p,q) &= f\ S_l(p,q) + (1-f)(S_k(p,q)\end{aligned}\right\}, \quad (5)$$

for $p = 1, 2, \ldots, i$; $q = 1, j$,

while for $p > i$, $q > j$, however,

$$\left.\begin{aligned} S_k'(p,q) &= S_k(p,q)\\ S_l'(p,q) &= S_l(p,q)\end{aligned}\right\}. \quad (6)$$

The mixing coefficient f is randomly chosen from a range $(0 < f < 1)$. We may point out that the specific form of crossover operation used here is dictated by the physics of the problem. Since the region near the nucleus is energetically important, it is necessary to ensure that amplitudes for small values of r ($r = 0 \leftrightarrow \infty$) are frequently sampled by the crossover operator (CO). The redefinition of the CO used here has been found to be beneficial[6]. After crossover, each of the children strings is subjected to a process of mutation with probability p_m. The site for mutation is chosen by comparing a random number $r[0, 1]$ with p_m for each pair of column and row indices (i, j). If for the kth string $r < p_m$ for $i = p$, $j = q$, the corresponding amplitude is mutated as follows:

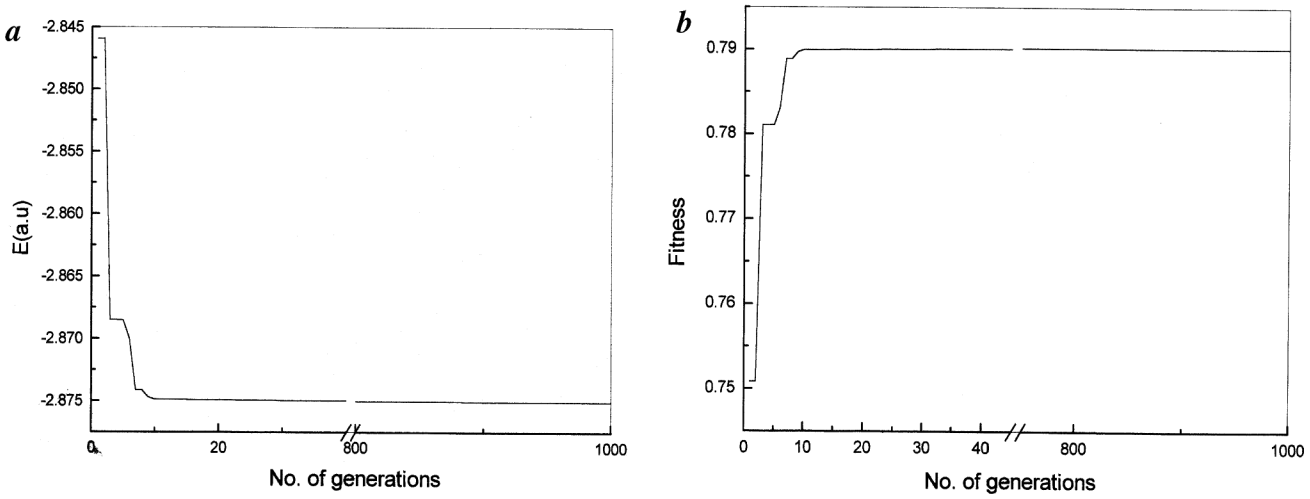

Figure 1. *a*, Evolution of energy of ground state of He atom during GA run. Energy refers to the string of the highest fitness in the population. *b*, Fitness profile during GA run for He atom in the ground state. Fitness corresponds to the string of the highest fitness in any generation.

$$S''_k(p, q) = S'_k(p, q) + (-1)^l r.\Delta_m, \tag{7}$$

where r is a random number ($0 \le r \le 1$), l is a random integer and Δ_m is the intensity of mutation. It may vary with generation or remain static[6].

The last operator to act on the post-crossover and post-mutation strings is the symmetrization operator, the action of which is defined as follows:

$$S'''_k(q, p) = S''_k(p, q), \text{ for } k = 1, 2, \ldots, \text{npop}, \tag{8}$$

for $p = 1, 2, \ldots, n_1$; $q = 1, 2, \ldots, n_2$; where 'npop' is the number of strings in the population.

With symmetrization, one generation is said to have elapsed. From the post-symmetrization population, we choose 80% of the strings in order of fitness and the remaining 20% are randomly created. The sequence of operations outlined is repeated till the average fitness of the population does not improve any more.

We report here the results of application of the method to the ground state of He atom. For this case ψ has been represented as amplitude distribution function on a two-dimensional grid of 20 a.u. of length in each dimension, each dimension having 500 uniformly distributed grid points. A string s_k thus carries 500×500 grid-point amplitudes which are allowed to evolve explicitly under the action of genetic operators, while the quadratures are performed over 1500×1500 grid-point amplitudes for more accurate evaluation of the integrals in eq. (4) for calculating the fitness of a string. The additional amplitudes are generated by two-dimensional bicubic interpolation. We have used a population size of ten throughout. The amplitude distributions on the 2D grid representing the strings were chosen from functions of the type

$$\psi = Ne^{-\beta(r_1+r_2)}\chi(r_{12}), \tag{9}$$

with $\chi(r_{12}) = 1 + \gamma r_{12} + \delta r_{12}^2 + \ldots$, with randomly chosen values of $\beta, \gamma, \delta, \ldots$. After the selection phase of evaluation is executed, a pair of strings is chosen randomly with crossover probability $p_c = 0.75$, for crossover. The mutation operation is then carried out on the post-crossover strings, followed by spatial symmetrization. Figure 1 *a* and *b* shows the energy and fitness profiles during the evolution of the strings representing the ground state wave function of helium atom. The major lowering of energy takes place in the first 15 generations. The rapid improvement of energy and therefore fitness in the early stages of evolution is dominated by the crossover operator. Towards the end of the evolution, improvement in fitness is dominated by mutation which accounts for slow improvement of the fitness values. The two-dimensional contour plot of the converged ground-state radial wave function of He atom obtained by GA is shown in Figure 2. Since this is an *S*-state and only radial correlation is present, the probability density is high in the near nucleus region. The energy corresponding to the best string is –2.87505 a.u. (1 a.u. of energy = 27.209 eV), which matches with ground state *s*-limit energy of He atom[10]. The energy obtained by GA is a bit lower than the Hartree–Fock energy of the He atom in the ground state. Results obtained so far indicate that the quality of results does not deteriorate with the increase of nuclear charge (z). The GA-based recipe described here is computationally at least as viable as numerical Hartree–Fock method for two-electron atoms. When the number of electrons (n) rises, the problem of performing multidimensional quadratures may prove to be a bottleneck. For $n > 2$, therefore, we must explore Monte Carlo methods for evaluating multidimensional integrals along with parallelization.

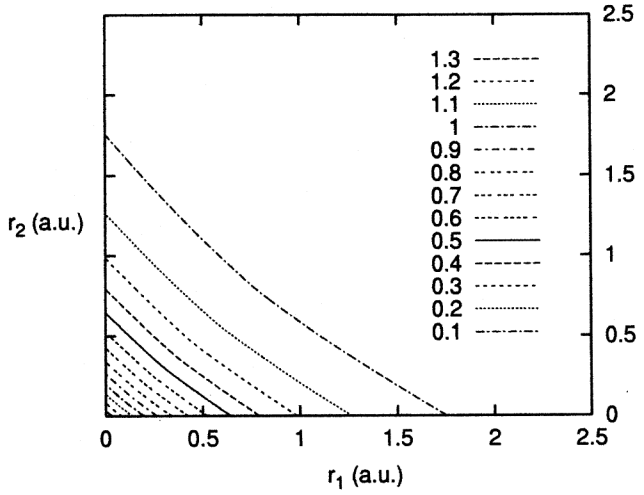

Figure 2. Two-dimensional contour plots of wave function amplitudes for He atom in the ground state.

We are in the process of completing the calculations on the entire helium sequence and extending the calculations to the fully correlated systems. We will shortly return to these results.

1. Holland, J. H., *Adaptation in Natural and Artificial Systems: An Introductory Analysis with Application in Biology, Control and Artificial Intelligence*, MIT, 1998.
2. Goldberg, D. E., *Genetic Algorithms in Search, Optimization and Machine Learning*, Addison Wesley, Reading, MA, 1989.
3. Chaudhury, P. and Bhattacharyya, S. P., Numerical solutions of the Schrödinger equation directly or perturbatively by genetic algorithm: test cases. *Chem. Phys. Lett.*, 1998, **296**, 51–60.
4. Makarov, D. E. and Metiu, H., Fitting potential energy surfaces: A search in the function space by directed genetic programming. *J. Chem. Phys.*, 1998, **108**, 590–598.
5. Makarov, D. E. and Metiu, H., Using genetic programming to solve the Schrödinger equation. *J. Phys. Chem.*, 2000, **A104**, 8540–8545.
6. Saha, R., Chaudhury, P. and Bhattacharyya, S. P., Numerical solution of Schrödinger equation by genetic algorithm. *Phys. Lett.*, 2001, **A291**, 397–406.
7. Nakanishi, H. and Sugawara, M., Numerical solution of the Schrödinger equation by a microgenetic algorithm. *Chem. Phys. Lett.*, 2000, **327**, 429–438.
8. Zeiri, Y., Fattal, E. and Kosloff, R., Application of genetic algorithm to the calculation of bound states and local density approximations. *J. Chem. Phys.*, 1995, **102**, 1859–1862.
9. Saha, R., Bhattacharyya, S. P., Christopher Taylor, Jhou, Y. and Cundari, T., Direct solution of the Schrödinger equation by a parallel genetic algorithm: Cases of an exactly solvable 2D interacting oscillator and the hydrogen atom. *Int. J. Quant. Chem.*, 2003, **94**, 243–250.
10. Davis, H. L., Radial limit in the configuration-interaction method for the 1's state of the helium isoelectronic sequence. *J. Chem. Phys.*, 1963, **39**, 1827–1832.

ACKNOWLEDGEMENT. We thank CSIR, New Delhi for research grant.

Received 15 September 2003; revised accepted 26 December 2003

Signature of early ozone hole recovery during 2002

S. L. Jain*, Sachin D. Ghude and B. C. Arya

Radio and Atmospheric Sciences Division, National Physical Laboratory, New Delhi 110 012, India

Total column ozone has been measured using Microtop Sunphotometer at Maitri (70°45′S, 11°44′E), Antarctica during the 21st Indian Antarctic Scientific Expedition. Observations show that the ozone hole in the year 2002 was not as deep as that of the previous few years. The minimum value of total ozone of about 185 DU was observed in the last week of September during 2002 and 135 DU during 1997. Observations also reveal the early recovery of ozone hole during 2002 compared to 1997. The Maitri observations were also compared with TOMs data as well as a nearby Russian station data and were found to be in good agreement.

OZONE is one of the most important constituents in the atmosphere and in spite of its low concentration, a few ppmv in mixing ratio, it plays an important role not only in the chemistry of this region, but it also affects the dynamics and biological activity near the surface. The amount of ozone over any particular place depends not only on photochemical balance, but also on the stratospheric climate, the winds that transport the ozone[1].

The reporting of catalytic depletion of ozone by ClO_x and NO_x by Johnston[2] in general, and ozone hole over Antarctica in particular by Farman *et al.*[3] has generated an unprecedented surge of interest in the scientific community in the monitoring of ozone. Very low temperature during winter leads to the formation of polar stratospheric clouds (PSCs)[4]. The heterogeneous chemical reactions that take place on the surface of the PSCs, are responsible for the ozone hole phenomenon during springtime over Antarctica[4]. Chemical reactions in the presence of liquid or ice particles either as ice or nitric acid trihydrate, or other mixtures lead to the conversion of chlorine compounds, which normally are present as HCl and $ClONO_2$ in the stratosphere. Normally, these gases do not react with ozone. However, in the presence of ice particles, HCl and $ClONO_2$ are converted into Cl_2 and HNO_3, and if UV-solar radiation is available, then Cl_2 is converted into Cl atoms, which then react with ozone to form ClO. Thereafter, a new chemical scheme, involving Cl_2O_2 as intermediate, comes into action, which destroys ozone efficiently[5–9].

However, planetary waves work against CFC-induced ozone destruction. These vast pressure waves influence ozone destruction in several ways and can have relevant impact on the size and stability of the massive jet stream

*For correspondence. (e-mail: sljain@mail.nplindia.ernet.in)